

This is an Open Access document downloaded from ORCA, Cardiff University's institutional repository:<https://orca.cardiff.ac.uk/id/eprint/110610/>

This is the author's version of a work that was submitted to / accepted for publication.

Citation for final published version:

Jiao, Yilai, Adedigba, Abdul-Lateef, He, Qian , Miedziak, Peter J., Brett, Gemma Louise, Dummer, Nicholas F. , Perdjon, Michal , Liu, Jinmin and Hutchings, Graham John 2018. Inter-connected and open pore hierarchical TS-1 with controlled framework titanium for catalytic cyclohexene epoxidation. *Catalysis Science and Technology* 8 , pp. 2211-2217. 10.1039/C7CY02571H

Publishers page: <http://dx.doi.org/10.1039/C7CY02571H>

Please note:

Changes made as a result of publishing processes such as copy-editing, formatting and page numbers may not be reflected in this version. For the definitive version of this publication, please refer to the published source. You are advised to consult the publisher's version if you wish to cite this paper.

This version is being made available in accordance with publisher policies. See <http://orca.cf.ac.uk/policies.html> for usage policies. Copyright and moral rights for publications made available in ORCA are retained by the copyright holders.



Inter-connected and open pore hierarchical TS-1 with controlled framework titanium for catalytic cyclohexene epoxidation

Yilai Jiao^{a, b, †}, Abdul-Lateef Adedigba^{a, †}, Qian He^a, Peter Miedziak^a, Gemma Brett^a, Nicholas F. Dummer^a, Micheal Perdjon^a, Jinmin Liu^b, Graham J Hutchings^{a, *}

A post-synthesis method was developed to reduce the extra-framework titanium (Ti) in TS-1 zeolites (Si/Ti ratio = 50), in which tetrapropylammonium hydroxide (TPAOH) aqueous solution was used to promote the dissolution, redistribution and recrystallization processes, and hence to convert amorphous Ti species into zeolitic phases. It was found that TPAOH could effectively convert the extra-framework Ti into framework Ti, and the TPAOH concentration influenced the pore structure significantly. Under lower TPAOH concentration (i.e. 0.05M - 0.4M), only closed meso-/macropore (grooves and hollow cavities) can be created in the TS-1 crystals. At an optimum concentration of 0.5 M TPAOH, open and connected hierarchical mesopore and macropore were created in the resulting TS-1 zeolites. Compared with the parent TS-1, the amount of extra-framework titanium was reduced significantly from 14.4 % to 0.3% and the meso-/macropore volume was increased from 0.014 to 0.168 cm³/g accordingly upon TPAOH post treatment. Along with the parent TS-1 zeolite, the developed hierarchical TS-1 zeolites were assessed in the catalytic epoxidation of cyclohexene. It was confirmed that the amount of framework titanium and hierarchical pore structure influenced the catalytic activity considerably. Closed porosity slightly improved the cyclohexene conversion, whereas the open-pore sample shows the optimum catalytic activity in cyclohexene conversion.

Introduction

Titanium silicalite-1 (TS-1), where titanium isomorphously replaces silicon in a tetrahedral site of the MFI silicalite lattice¹, has attracted much attention due to its excellent catalytic oxidation properties. In many oxidation processes such as ammoxidation of cyclohexanone^{2, 3}, hydroxylation of phenol⁴, and epoxidation of olefins⁵⁻⁷, and under mild reaction conditions with hydrogen peroxide as the oxidant, TS-1 is an effective catalyst.

In TS-1 crystals there exist two types of titanium species, the framework and the extra-framework titanium. Typically, the framework titanium is the active site for epoxide production during epoxidation reactions, whereas the extra-framework titanium species are responsible for secondary and often unwanted reactions⁸. The extra-framework titanium species include anatase and rutile-type titanium dioxide (TiO₂) and amorphous titanium species, which will decompose H₂O₂ and lead to side reactions, such as hydrolysis and ring opening of the epoxide⁹⁻¹¹.

The traditional synthesis method of TS-1 inevitably produces extra-framework titanium, particularly when synthesizing TS-1 with low silicon to titanium ratios¹²⁻¹⁴. In addition, due to the microporous structure of this MFI zeolite, which has large diffusion resistance in the crystal, only active sites on the crystal surface and at the pore mouth can participate in many reactions, which results in a lower utilization of the catalyst active sites¹⁵⁻¹⁹. Therefore, to increase the catalytic performance of TS-1 catalyst, two key technical problems should be addressed. Firstly, TS-1 should be prepared with more active sites and less extra-framework titanium, and secondly diffusion and steric hindrances in the crystal should be minimized.

At present, the commonly used method for the modification of TS-1 is the post-synthesis treatment with sodium hydroxide to create mesopores, which act to improve diffusion and to reduce steric hindrance. Although sodium hydroxide can create mesopores in MFI zeolites it also decreases their relative crystallinity, and in addition increases the amount of extra-framework titanium in the TS-1²⁰⁻²². Recently, organic templates such as tetrapropyl ammonium hydroxide (TPAOH)²³⁻²⁶ and a mixture of TPAOH and NaOH²⁷ have been used to treat TS-1 after synthesis to obtain hollow TS-1. The TPAOH acts as an alkaline and dissolves the zeolite crystals to create mesopores in the TS-1 crystals. Also, the TPAOH can act as a template to recrystallize the dissolved zeolitic species to form new crystals. Due to the above dissolution-recrystallization process, the relative zeolite crystallinity is preserved better than what is obtainable with sodium hydroxide treatment. However, the above methods inevitably break the Si-O-Ti bonds in the crystal and convert part of the framework titanium to extra-framework titanium^{10, 23, 25}. Furthermore, the above methods produce a closed-pore meso-/macropore in the zeolites, with a dense shell around the crystal. In the use of such hollow TS-1 in liquid phase reactions involving bulky molecules, it is always difficult for the bulky molecule to easily diffuse through the crystal, which limits their reactivity to external and pore-mouth active sites. Therefore, optimization of the TPAOH post-treatment conditions is highly desirable to simultaneously create an open-pore (rather than just hollow cavities) and decrease extra-framework titanium in TS-1 zeolites while preserving their crystallinity.

^a Cardiff Catalysis Institute, School of Chemistry, Cardiff University, Park Place, Cardiff, CF10 3AT, United Kingdom.

^b Shenyang National Laboratory for Materials Science, Institute of metal Research, Chinese Academy of Sciences, Shenyang 110016, China.

* Corresponding Author: Hutch@cardiff.ac.uk

† Y. Jiao and A. Adedigba contributed equally to this work.

Electronic Supplementary Information (ESI) available: [details of any supplementary information available should be included here]. See DOI: 10.1039/x0xx00000x

Hence, the aim of this work is to produce a hierarchical TS-1 zeolite with connected and open mesopores with minimal extra-framework titanium species. The procedure includes the dissolution, recrystallization and redistribution/reinsertion of any extra-framework titanium species in the pristine sample to the framework positions by the treatment with TPAOH at elevated temperatures. To achieve the optimal balance between the amount and structure of the induced porosity, the reinsertion of the extra-framework species and the crystallinity of the final material, it is imperative to accurately obtain a balance between the dissolution and recrystallization steps. In this work the determination of the optimal TPAOH concentration to obtain an open-pore hierarchical material, and to minimize or eliminate any extra-framework titanium in the samples is reported. Cyclohexene epoxidation was used to evaluate the catalytic activities of the modified TS-1 materials and the results are related to the degree of reinserted titanium and the nature of the induced porosity. All the samples were characterized to determine the crystallinity, the extra/framework titanium content, mesopore size and distribution, and the crystal size.

Experimental methods

Synthesis of TS-1

Tetraethyl orthosilicate (TEOS), titanium (IV) ethoxide (TEOT), and tetrapropyl ammonium hydroxide (TPAOH, 25 wt. % in water) – used without further purification – acted as the silica, titanium, and the organic structure directing agents, respectively. The molar composition of the synthesis solution was SiO_2 : 0.02TiO_2 : 0.3TPAOH : $19\text{H}_2\text{O}$. The typical preparation procedures were as follows: Firstly, titanium (IV) ethoxide was added to TEOS under vigorous stirring, this solution was continually stirred for 1 hour. Then, a solution composed of the desired amount of TPAOH and deionized water was added drop-wise into the above solution under vigorous stirring. The mixture was stirred for 40 minutes at room temperature, then heated to 313 K under continuous stirring to remove alcohol and to obtain the synthesis gel. The synthesis gel was transferred into a Teflon-lined stainless steel autoclave for crystallization at 160°C for 48 hours. The product was recovered by centrifugation and washed with deionized water – the washing was accomplished by dispersing the solid products in 100 mL of water followed by separation 3 times – dried at 110°C and followed by calcination in static air at 550 °C with a ramp rate of 1 °C/min for 6 hours.

TPAOH Post-treatment

The TPAOH post-treatment was carried out as follows, 2 g of the as-prepared TS-1 (AP) was mixed with a 20 mL solution of TPAOH (0.05–0.5 mol/L) at 400 rpm for 20 minutes to form a slurry. The slurry was transferred to a Teflon-lined stainless steel autoclave, and treated under autogenous pressure at 160 °C for 24 hours. Finally, the mixture was filtered, washed with deionized water, dried at 120 °C for 12 hours, and calcined at 550 °C for 6 hours. The samples obtained were denoted as TT-x, in which x represented the molar concentration of TPAOH.

Catalytic performance testing

The epoxidation of cyclohexene used as the test reaction was carried out in a colaver glass reactor. Typically, 100 mg of catalyst, 6 mmol of reactant, 6 mmol of hydrogen peroxide (H_2O_2 , 30%), and 10 mL of solvent (acetonitrile) were added and stirred (800 rpm) at 333 K for 4 hours, after which the reactor was quenched in an ice bath for 20 minutes. The catalyst was separated from the product by filtering through a 0.45 μm PTFE syringe filter. The products of the reactions were analyzed using a gas chromatograph (Agilent 7890B) equipped with a flame ionization detector (FID) and Agilent CP76581 CP-Wax 52 CB column with dimensions of 25 m*0.53 mm*2 μm . The carbon balance is above 95%.

Characterization

Powder X-ray diffraction (XRD) was recorded using a PANalytical X'Pert Pro system fitted with a $\text{CuK}\alpha 1$ X-ray source operated at 40 kV and 40 mA. Each sample was scanned from $2\theta = 5^\circ$ to 35° for 30 minutes. A JEOL 7401 high-resolution field emission scanning electron microscope with an energy dispersive X-ray spectrometer (EDX) was used to image and analyze the silicon to titanium ratio of the catalysts. A JEOL 1010 and FeiTecnaif20 Transmission Electron microscope was used to carry out HR-STEM. The samples were prepared for TEM by placing a droplet of the powder dispersed in ethanol (sonicated for 5 min in an ultrasonic bath) on a carbon-coated mesh grid. The specific surface area and pore structure of the as-prepared and modified samples were determined by nitrogen (N_2) adsorption–desorption measurements at the liquid nitrogen temperature (77 K) using a Micromeritics 3flex Surface Area and pore size analyzer. The micropore size distribution was calculated by the Horvath-Kawazoe (HK) method, and mesopore and macropore distribution was determined from the adsorption branch of the isotherms by the Barrett-Joyner-Halenda (BJH) method. The meso-/macropore sizes of the catalysts were also analyzed using mercury (Hg) intrusion porosimetry on a Micromeritics' AutoPore IV 9510 (pressure range: 0.10 to 60000 psia). The UV–Vis and infrared (FTIR) spectra were recorded on a Shimadzu UV-2550 340 spectrophotometer and a Nicolet NEXUS 670 FT-IR spectrometer respectively.

Results and discussion

Crystallinity

The XRD patterns of the as-prepared and TPAOH treated samples are shown in Fig. 1. The five characteristic peaks of the MFI topology at 7.8° , 8.8° , 23.0° , 23.9° and 24.4° were identified in the as-prepared and TPAOH treated samples, and the peak at 24.4° , which is a singlet also indicates the crystal is typical of TS-1. The relative crystallinity, calculated by comparing the total intensity of the peaks from 22.5° to 24.6° with that of each sample is given in Table 1. Following the post-synthesis treatment with TPAOH, the relative crystallinity increased with increasing TPAOH concentration. The highest relative crystallinity was obtained for the sample treated with 0.3M TPAOH, TT-0.3M. Further increasing the TPAOH concentration results in a slightly decreased relative crystallinity.

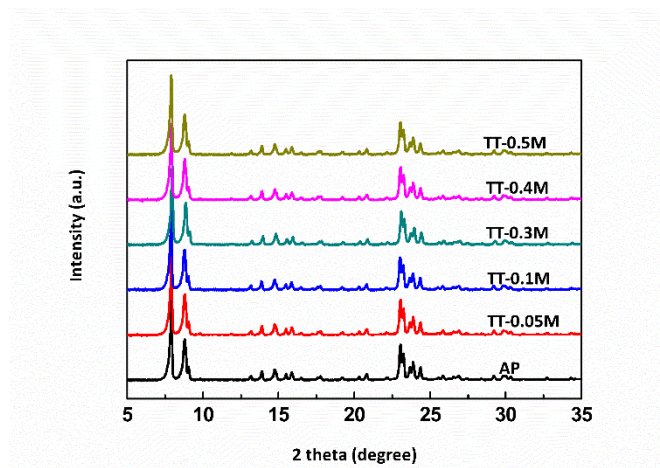


Figure 1. XRD pattern of as-prepared and samples treated with different TPAOH concentrations

The treatment of the zeolite with a base can cause the dissolution of zeolite, and in the presence of TPAOH and heat treatment recrystallisation can be induced. The dissolution and recrystallisation process can lead to the re-insertion of some amorphous silica and extra-framework titanium species into the zeolite framework, so that the relative crystallinity is enhanced. Although, increasing the TPAOH concentration will speed up the above process, at higher TPAOH concentrations the silica and titanium concentration in the solution will be significantly high, and result in a slight decrease in the relative crystallinity.

Textural properties

The type I isotherms of the as-prepared sample measured by N_2 adsorption (Fig. 2a) confirm their microporous character. The as-prepared samples treated in TPAOH solution under hydrothermal conditions show a combined type I and type IV isotherm, which is characteristic of a hierarchical porous system with a combination of both micro- and mesoporosity. The details of the textural properties of the sample treated with different TPAOH concentration are summarized in Table 1. With increasing TPAOH concentration, the mesopore surface area and mesopore volume can be seen to increase. The highest micropore surface area ($442 \text{ m}^2\text{g}^{-1}$) and total pore volume ($0.338 \text{ cm}^3\text{g}^{-1}$) were obtained when the sample was treated with 0.5M TPAOH. In addition, the as-prepared TS-1 and TPAOH modified samples have similar micropore distribution, which confirms the process of dissolution-recrystallization (Figure S1a, b). The BJH pore size distribution of the TPAOH treated samples shows random mesopores and macropores in the range 10 nm to 160 nm (Figure 2b and Figure S1c), and the pore size increase with the concentration of TPAOH.

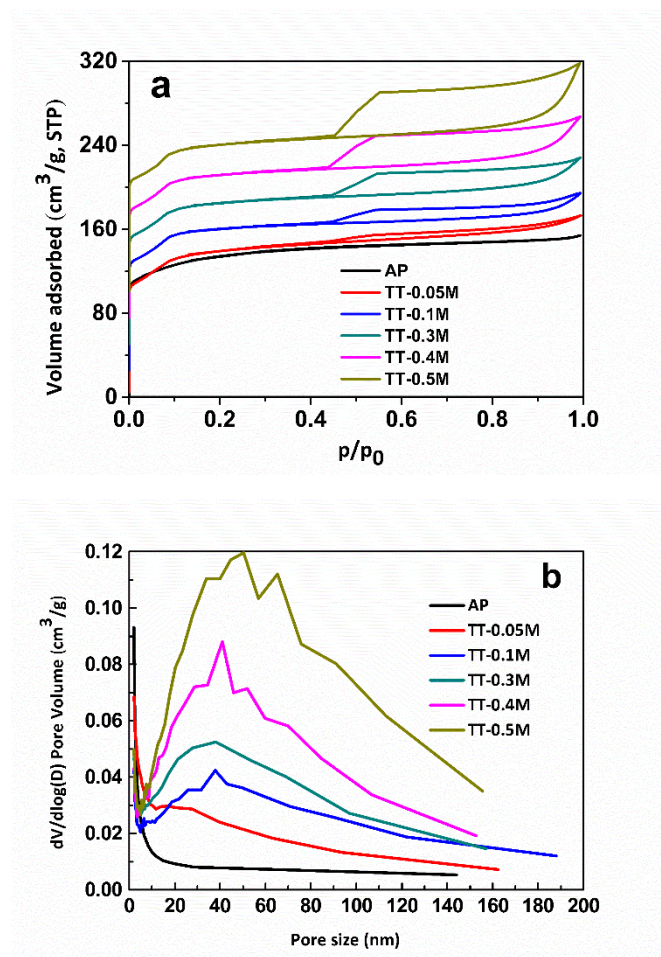


Figure 2. N₂ adsorption–desorption isotherms (a) and BJH pore size distribution (b) of as-prepared and TPAOH treated samples

In liquid phase reactions, the diffusivity of species is generally five orders of magnitude slower than that in the gas phase²⁸, hence, open porosity (mesopore and macropore) is advantageous as it will facilitate molecular diffusion and increase the accessibility to the active sites that are located in the microporous channels from the outside^{29, 30}. As N₂ sorption only provides the total porosity – including both open and close porosity – a complementary method is required to discriminate between the open and closed mesopore and macropores.

To complement the porosity of samples AP, TT-0.4M and TT-0.5M obtained by N₂ sorption, mercury porosimetric measurements were performed. The Hg intrusion technique was selected to distinguish between the open and close pores

Table 1. Summary of the properties of as-prepared (AP) and TPAOH modified (TT-XM) TS-1 samples

Sample	Relative crystallinity [%]	Si/Ti	S _{BET} [m ² g ⁻¹]	S _{micro} ^a [m ² g ⁻¹]	S _{external} ^a [m ² g ⁻¹]	V _{micro} ^a [cm ³ g ⁻¹]	V _{t-m} ^b [cm ³ g ⁻¹]	V _t [cm ³ g ⁻¹]
AP	91.0	46	495	462	33	0.168	0.014	0.182
TT-0.05M	97.0	42	495	414	81	0.174	0.088	0.262
TT-0.1M	97.9	44	500	416	84	0.173	0.089	0.262
TT-0.3M	100	42	497	413	84	0.172	0.104	0.276
TT-0.4M	99.6	42	506	423	83	0.175	0.123	0.298
TT-0.5M	99.1	44	549	442	107	0.170	0.168	0.338

^at-plot method; ^bCalculations were based on total pore volume minus micropore volume

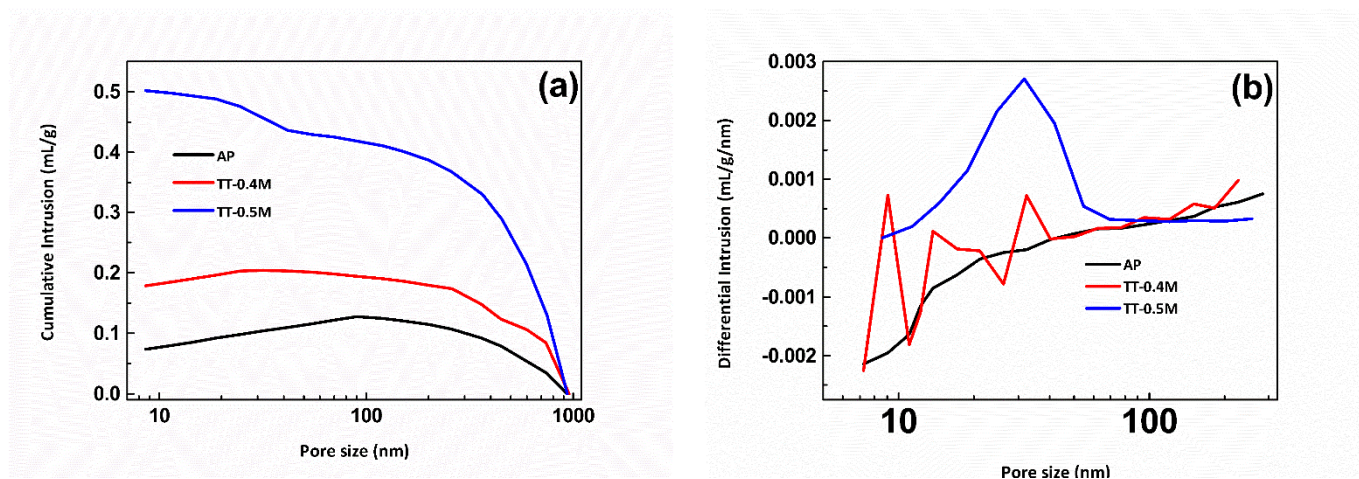


Figure 3. Mercury porosimetric measurements for sample AP, TT-0.4M and TT-0.5M (a) cumulative intrusion, (b) pore size distribution

because Hg cannot significantly penetrate pores smaller than 3 nm³¹. Hence, for Hg to successfully intrude the inner pores from the exterior, the external pore through which it accesses the interior must be large enough (> 3nm) and it will imply that the internal meso/macropores are open through to the exterior from where the Hg intrudes. The Hg intrusion and pore size distribution curves are shown in Fig. 3. From figure 3a, an obvious increase from 10 nm to 50 nm can be seen in sample TS-0.5M, confirming that the mesopore and macropore in TT-0.5M are open to the external zeolite surface. Also, an obvious peak in this pore range can be seen in figure 3b for sample TT-0.5M, whereas sample TT-0.4M only displays random peaks in the same pore region, which implies that the Hg cannot intrude into the crystals of the sample TT-0.4M thereby resulting in the collapse.

Morphology

The SEM images of the as-prepared and TPAOH modified samples are shown in Figure 4. There are no obvious differences between the AP sample and the TPAOH modified samples. All the samples have almost uniform particle size of approximately 500 nm. The silicon to titanium ratio of the samples before and after TPAOH treatment evaluated by EDS is given in Figure S2. From the EDS analysis, after TPAOH treatment, the silicon to titanium ratio decreased slightly from 46 to 42 (Table S1), which further confirms the dissolution-recrystallisation process with TPAOH treatment.

The nature and structure of the mesopore in the treated samples was further evaluated by the TEM, and is shown in Figure 5. The as-prepared microporous TS-1 crystal displayed a dark image (Fig. 5a), and as expected, some large voids can be seen in the inner part of the zeolite crystals treated with 0.1 M of TPAOH (Fig. 5b). Compared to the samples treated with 0.1M TPAOH, a higher quantity of voids can be seen in the sample that was treated with 0.4M TPAOH solution (Fig. 5c). However, from the higher magnification image (Figure 5d), we can see that the voids in the sample was covered by a dense shell. On the contrary, the pore structure in the sample that was treated with 0.5 M TPAOH solution was open to the surface (Figure 5e, f). Furthermore, the mesopore and macropore in TT-0.5M are interconnected and exposed to the crystals external surface (Figure S3b). The above results are complimentary to the results of the mercury intrusion, and confirm the open hierarchical porosity in TT-0.5M. The selected area electron diffraction (SAED) patterns of 0.1M, 0.4M and 0.5M TPAOH treated samples (Figure S4b, c and d) are similar to that of the as-prepared sample (Fig. S4a), which also support the conclusion that the TPAOH treatment do not destroy the crystallinity of the as-prepared sample contrary to those of desilication by NaOH²².

To determine the onset of the open pore structure and to assess if the open pore can be sustained beyond 0.5M, the as-prepared sample was treated with 0.45M and 0.6M solutions of TPAOH. Figure S3a and S3e show the TEM images of these two samples and confirm that concentrations of TPAOH higher than 0.4M were required to induce the open-pore structure. The TT-0.6M maintains an open pore structure and the parent morphology beyond 0.5M TPAOH concentrations.

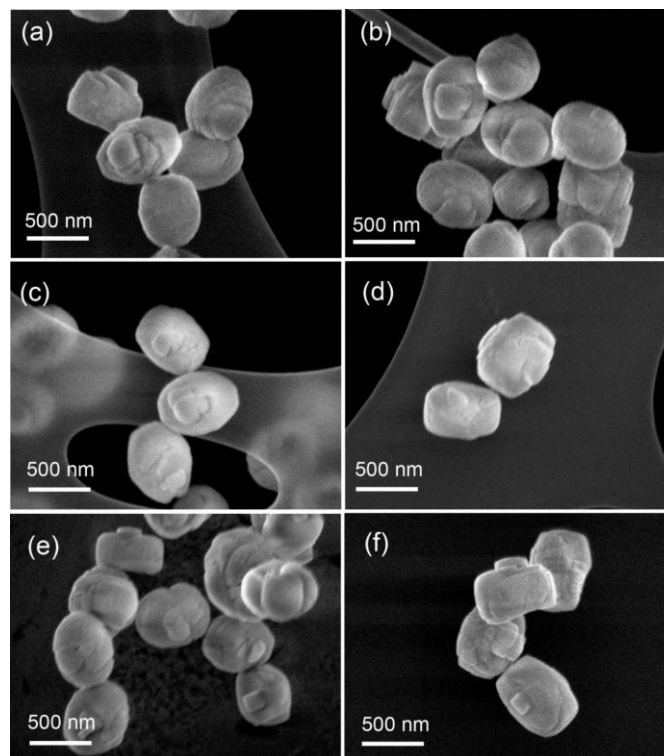


Figure 4. SEM images of as prepared and TPAOH treated samples (a) as prepared TS-1, (b) TT-0.05M, (c) TT-1-0.1M, (d) TT-0.3M, (e) TT-0.4M and (f) TT-0.5M

The nature of the Titanium composition

The FTIR and the diffuse reflectance UV-Vis were used to evaluate the nature of the titanium species on both the original and modified zeolite samples. As shown in Fig. 6, all the samples including those treated with TPAOH retain the band at 960cm^{-1} , which is attributable to titanium in the framework position. The presence of titanium in the framework position can be inferred from the FTIR analysis of TS-1 samples as represented in Fig. 6, however, the existence of extra-framework species cannot be detected with the FTIR.

To identify extra-framework titanium in the as-prepared and TPAOH treated samples, and to monitor the role of the post-treatment conditions on the titanium distribution, UV-Vis analysis was used (Fig. 7). The samples show a transition at approximately 210 nm characteristic of framework titanium species, which correlates with the results in Fig. 6. In addition to the 210 nm transition, all the samples also exhibit an additional transition at around 300 nm, which is characteristic of extra-framework titanium species⁸. Importantly, the intensity and shape of the peak at about 300 nm for the different treated samples differs. The as-prepared sample displayed the highest and broadest peak at 300 nm in the series, and with increasing TPAOH concentrations, the transition at 300 nm reduces, which suggests that the extra-framework titanium content in the samples is reduced, which demonstrates the dissolution, recrystallization and redistribution of the titanium species. The titanium amount in the as-prepared sample and TPAOH modified samples was calculated from the peak area of the UV-Vis curve. The as-prepared sample comprised of approximately 85.6% framework titanium, whereas upon treatment with TPAOH the framework titanium content increased gradually to 92.1% (0.05M), 98.5% (0.1M), 99.5% (0.3M), 97.8% (0.4M) and 99.7% (0.5M), another evidence to support the dissolution, recrystallization and redistribution of the titanium species.

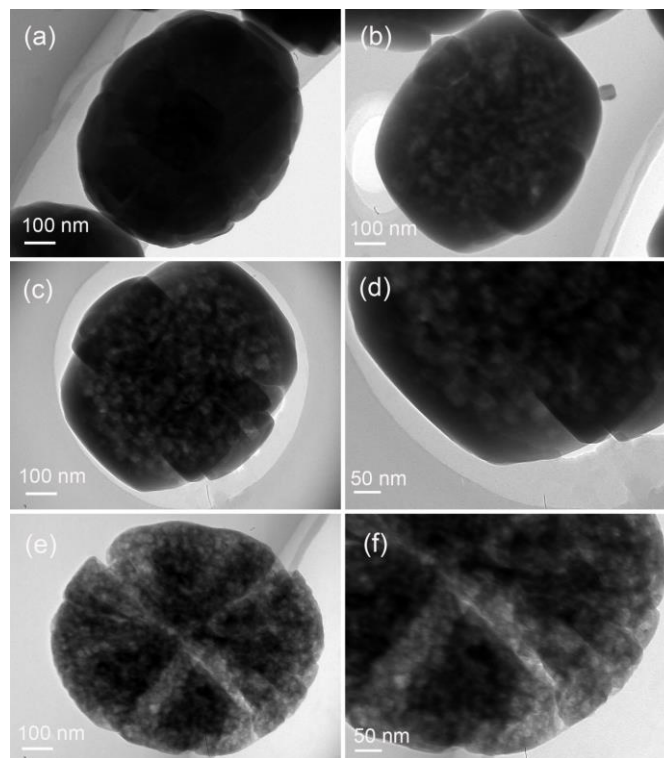


Figure 5. TEM images of as prepared and TPAOH treated samples (a) as prepared TS-1, (b) TT-0.1M, (c, d) TT-0.4M and (e, f) TT-0.5M

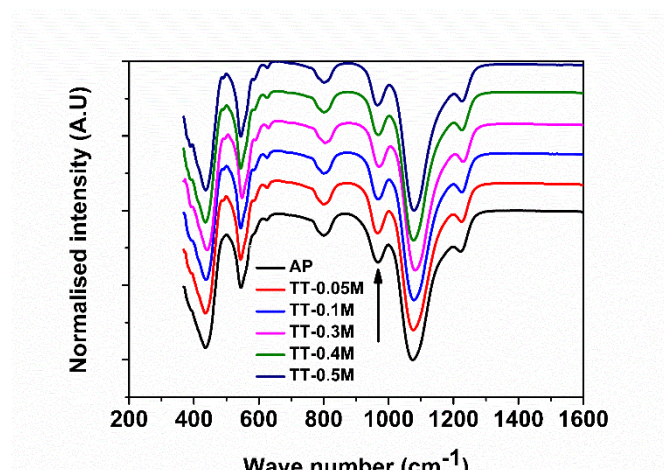


Figure 6. FTIR spectra of as-prepared and TPAOH modified samples. The arrow indicate the 960 cm^{-1} position that indicates framework titanium species

These results differ from those of previous studies where the relative crystallinity decreased and the amount of framework titanium increased after TPAOH treatment^{27, 32, 33}. The reason for such disparity we reckon is due to the low TPAOH concentration used in those studies, typically 0.005M to 0.1M. Similarly, such low TPAOH concentration were effective in creating groves and hollow cavities in the TS-1 but were not able to initiate open-pore meso-/macropore and that could be the reason why some reseachers³³ have noticed no influence of the created mesopore on activity. It shows that the post treatment condition, namely TPAOH concentration must be carefully selected to obtain open-pore hierarchical TS-1.

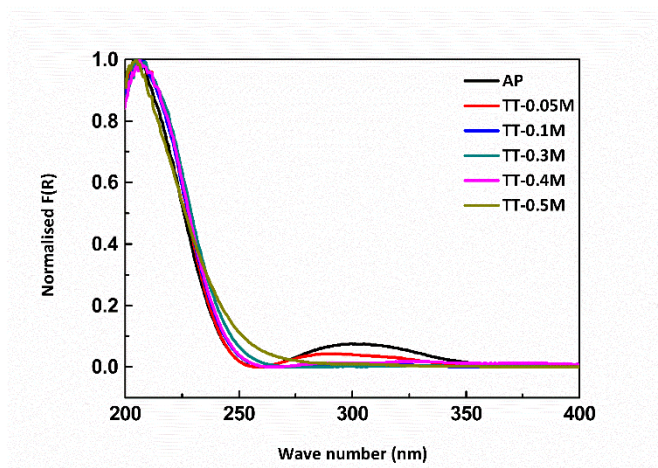


Figure 7. UV-Vis analysis of as prepared and TPAOH modified samples. The spectra are normalised to the same scale to ensure accurate and representative direct comparison

Cyclohexene epoxidation performance

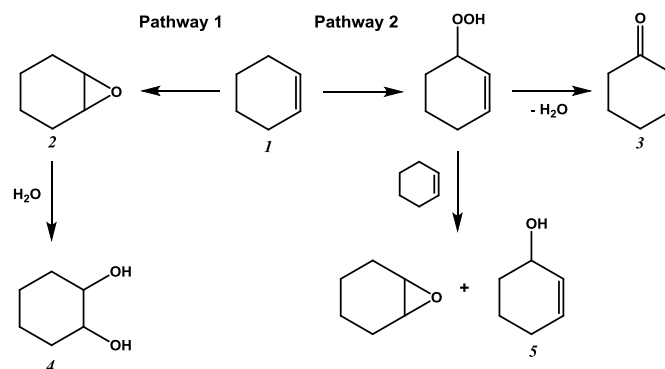
The influence of the titanium distribution and the induced hierarchical porosity of the treated samples were evaluated with cyclohexene epoxidation. Table 2 shows the results of the catalytic activity and the product distribution over each sample. As expected the as-prepared sample exhibited the least activity compared to the TPAOH treated samples, and the sample treated with 0.5M TPAOH showed the highest activity, while the other TPAOH treated samples display similar activity, which is higher than the pristine sample. The activity of the sample treated with 0.5M TPAOH doubles (19%) that of the other treated samples (10%). The marked difference in the activity between TT-0.5M and other treated samples can be correlated with the structure of the induced meso-/macropores in the samples. At concentrations of TPAOH lower than 0.5M, only closed mesopores and macropores or hollow cavities were present, which means the active sites are only those on the catalyst surface and at a few distances below the pore mouth. However, and as observed in Fig. 3 and 5, TT-0.5M have open and inter-connected meso-/macropores offering access to more active sites both on the surface and within the inner pores. In addition, the steric and diffusion limitation on TT-0.5M would be lower than the others due to the inter-connectivity and the open nature of its pores.

The product distribution of the as-prepared and modified samples is also given in table 2. Generally, there are two pathways to convert cyclohexene according to the proposed scheme by Kwon *et al.*²⁶ – given in scheme 1. Firstly, cyclohexene (**1**) is epoxidized to cyclohexene oxide (**2**), which can be hydrolysed to 1,2-cyclohexanediol (**4**) under acidic conditions²⁶. The other pathway is the allylic oxidation of cyclohexene to cyclohexen-1-one (**3**) and 2-cyclohexen-1-ol (**5**). Compared with the as-prepared sample, the TPAOH modified samples have a comparable selectivity to cyclohexene oxide, while the TPAOH modified samples have higher selectivity of 1,2-cyclohexanediol and lower selectivity of cyclohexen-1-one and 2-cyclohexen-1-ol. This implies that more cyclohexene is oxidized to cyclohexene oxide and 1,2-cyclohexanediol via *Pathway 1* over the TPAOH modified samples when compared to over the as-prepared sample. These results clearly demonstrate the positive role of framework titanium in promoting *Pathway 1* as the primary reaction route.

Table 2. Cyclohexene conversion and product selectivity over the as-prepared and TPAOH treated samples

Sample	Cyclohexene conversion [%]	Selectivity [%]		
		Cyclohexene epoxide	1,2-cyclohexanediol	Cyclohexen-1-one and 2-cyclohexen-1-ol
AS	6.5	82.3	10.2	7.5
TT-0.05M	10.2	78.3	16.4	5.3
TT-0.1M	9.6	81	14.7	4.3
TT-0.3M	10	77	18.2	4.8
TT-0.4M	11	82	15	3
TT-0.5M	19	78	17	5

Reaction conditions; Cyclohexene: 6 mmol, 30 wt% H₂O₂: 6 mmol, Catalyst: 100 mg, temperature: 60 C, reaction time: 4 h



Scheme 1. Schematic of cyclohexene (1) oxidation with hydrogen peroxide²⁶

Conclusions

In conclusion, open-pore hierarchical TS-1 type zeolites with high mesopore and macropore volume and controlled framework titanium was synthesized by a combination of TPAOH and temperature post-treatment. This method allows the dissolution, redistribution and recrystallization of the treated samples allowing the preservation of the crystallinity and the reinsertion of the extra-framework titanium into the framework positions. We demonstrated that the TPAOH concentration influences the extent to which the extra-framework titanium is reinserted to the framework position, and the mesopore and macropore volume, and structure. It was found that 0.5 M TPAOH efficiently promoted the effective conversion of extra-framework titanium to framework position in addition to inducing high volume of mesopore and macropore that are inter-connected and open to the external surface, which promoted a high cyclohexene conversion. The TPAOH treated samples all show selectivity to epoxide similar to that of the as-prepared samples, which demonstrate the efficiency of this technique in mitigating against the extra-framework titanium species.

Conflicts of interest

There are no conflicts to declare

Acknowledgements

YJ thanks the China Scholarship Council (CSC) for his fellowship in the UK (201604910181). YL also thanks Dr Greg Shaw for UV-Vis training, Dr Thomas Davies for TEM training.

References

1. A. Thangaraj, R. Kumar, S. P. Mirajkar and P. Ratnasamy, *Journal of Catalysis*, 1991, 130, 1-8.
2. A. Thangaraj, S. Sivasanker and P. Ratnasamy, *Journal of Catalysis*, 1991, 131, 394-400.
3. A. Zecchina, S. Bordiga, C. Lamberti, G. Ricchiardi, C. Lamberti, G. Ricchiardi, D. Scarano, G. Petrini, G. Leofanti and M. Mantegazza, *Catalysis Today*, 1996, 32, 97-106.
4. A. Thangaraj, R. Kumar and P. Ratnasamy, *Journal of Catalysis*, 1991, 131, 294-297.
5. R. Meiers, U. Dingerdisen and W. F. Hölderich, *Journal of Catalysis*, 1998, 176, 376-386.
6. M. G. Clerici, G. Bellussi and U. Romano, *Journal of Catalysis*, 1991, 129, 159-167.
7. M. G. Clerici and P. Ingallina, *Journal of Catalysis*, 1993, 140, 71-83.
8. P. Ratnasamy, D. Srinivas and H. Knözinger, in *Advances in Catalysis*, Academic Press, 2004, vol. 48, pp. 1-169.
9. G. Xiong, Y. Cao, Z. Guo, Q. Jia, F. Tian and L. Liu, *Physical Chemistry Chemical Physics*, 2016, 18, 190-196.
10. Y. Zuo, M. Liu, T. Zhang, L. Hong, X. Guo, C. Song, Y. Chen, P. Zhu, C. Jaye and D. Fischer, *RSC Advances*, 2015, 5, 17897-17904.
11. G. Xiong, Q. Jia, Y. Cao, L. Liu and Z. Guo, *RSC Advances*, 2017, 7, 24046-24054.
12. A. Tuel, *Catalysis Letters*, 1998, 51, 59-63.
13. N. Wilde, M. Pelz, S. G. Gebhardt and R. Glaser, *Green Chemistry*, 2015, 17, 3378-3389.
14. M. Tamura, W. Chaikittisilp, T. Yokoi and T. Okubo, *Microporous and Mesoporous Materials*, 2008, 112, 202-210.
15. Y. Jiao, X. Fan, M. Perdjon, Z. Yang and J. Zhang, *Applied Catalysis A: General*, 2017, 545, 104-112.
16. X. Ou, S. Xu, J. M. Warnett, S. M. Holmes, A. Zaheer, A. A. Garforth, M. A. Williams, Y. Jiao and X. Fan, *Chemical Engineering Journal*, 2017, 312, 1-9.
17. Y. Jiao, X. Yang, C. Jiang, C. Tian, Z. Yang and J. Zhang, *Journal of Catalysis*, 2015, 332, 70-76.

18. Y. Jiao, C. Jiang, Z. Yang and J. Zhang, *Microporous and Mesoporous Materials*, 2012, 162, 152-158.
19. Y. Jiao, C. Jiang, Z. Yang, J. Liu and J. Zhang, *Microporous and Mesoporous Materials*, 2013, 181, 201-207.
20. V. Valtchev, G. Majano, S. Mintova and J. Perez-Ramirez, *Chemical Society Reviews*, 2013, 42, 263-290.
21. X.-Y. Yang, L.-H. Chen, Y. Li, J. C. Rooke, C. Sanchez and B.-L. Su, *Chemical Society Reviews*, 2017, 46, 481-558.
22. A. Silvestre-Albero, A. Grau-Atienza, E. Serrano, J. García-Martínez and J. Silvestre-Albero, *Catalysis Communications*, 2014, 44, 35-39.
23. B. Wang, M. Lin, X. Peng, B. Zhu and X. Shu, *RSC Advances*, 2016, 6, 44963-44971.
24. M. Lin, C. Xia, B. Zhu, H. Li and X. Shu, *Chemical Engineering Journal*, 2016, 295, 370-375.
25. T. Zhang, Y. Wang, S. Wang, X. Wu, P. Yao, W. Feng, Y. Lin and J. Xu, *Reaction Kinetics, Mechanisms and Catalysis*, 2015, 114, 735-752.
26. S. Kwon, N. M. Schweitzer, S. Park, P. C. Stair and R. Q. Snurr, *Journal of Catalysis*, 2015, 326, 107-115.
27. B. Wang, M. Lin, B. Zhu, X. Peng, G. Xu and X. Shu, *Catalysis Communications*, 2016, 75, 69-73.
28. X. Ou, X. Zhang, T. Lowe, R. Blanc, M. N. Rad, Y. Wang, N. Batail, C. Pham, N. Shokri, A. A. Garforth, P. J. Withers and X. Fan, *Materials Characterization*, 2017, 123, 20-28.
29. J. García-Martínez and K. Li, eds., *Mesoporous Zeolites: Preparation, Characterization and Applications*, Wiley-VCH, Weinheim, Germany, 2015.
30. D. Verboekend, N. Nuttens, R. Locus, J. Van Aelst, P. Verolme, J. C. Groen, J. Perez-Ramirez and B. F. Sels, *Chemical Society Reviews*, 2016, 45, 3564-3564.
31. J. C. Groen, S. Brouwer, L. A. A. Peffer and J. Pérez-Ramírez, *Particle & Particle Systems Characterization*, 2006, 23, 101-106.
32. G. Wu, Z. Lin, L. Li, L. Zhang, Y. Hong, W. Wang, C. Chen, Y. Jiang and X. Yan, *Chemical Engineering Journal*, 2017, 320, 1-10.
33. X. Wu, Y. Wang, T. Zhang, S. Wang, P. Yao, W. Feng, Y. Lin and J. Xu, *Catalysis Communications*, 2014, 50, 59-62.